Radiation Physics and Chemistry 220 (2024) 111648

Contents lists available at ScienceDirect

Radiation Physics and Chemistry

journal homepage: www.elsevier.com/locate/radphyschem

Understanding the X-ray emission spectrum after excitation with a source of X-rays: From theory to experiment

Jorge E. Fernández [a,*], Gianmarco Grippo [a], Francesco Teodori [a], Viviana Scot [b]

[a] Laboratory of Montecuccolino-DIN, Alma Mater Studiorum University of Bologna, Via Dei Colli 16, 40136 Bologna, Italy
[b] Nier SpA Via Clodoveo Bonazzi, 2, 40013 Castel Maggiore, Italy

ARTICLE INFO

Handling Editor: Dr. Chris Chantler

ABSTRACT

The modified Boltzmann-Chandrasekhar equation of transport for photons is the proper framework for describing the photon radiation field with a complete description of the polarization state. The characterization of the radiation field requires a detailed knowledge of the interactions of photons with mater and comprises also the contribution of the secondary electrons to the photon field through mechanisms like inner impact ionization and bremsstrahlung. It will be shown a solution obtained without the need of solving the coupled transport electrons-photons. With all these interactions, the theoretical characterization of the X-ray spectrum of emission after excitation with a source of X-rays can be straightforwardly obtained from the albedo solution to the equation. In this work it will be privileged a Monte Carlo (MC) solution. However, this solution is still far from an experimental measurement modified by the radiation detection devices, comprised the pulse electronics. In this work we put together a MC simulation able to get a detailed transport solution and a complete characterization of the contributions of the detection chain. It is discussed the influence of the single contributions and how they combine to make that a simulated X-ray spectrum matches well a real measurement.

1. Introduction

It is well known that the measured intensity $I_{measured}(E)$ (Seltzer, 1981) and the modification due to the detector are linked through the convolution integral

$$I_{measured}(E) = \int R(E^{'}, E)\varphi(E^{'})I(E^{'})dE^{'}, \tag{1}$$

where $R(E^{'}, E)$ denotes the detector response for an incident photon with energy $E^{'}$, $\varphi(E^{'})$ the detector efficiency and $I(E^{'})$ the source intensity at the same energy. It is worth noting that sometimes the efficiency is comprised into the response function. In this paper we prefer to show it separately for reasons which will be clear later.

The detector response function

$$R(E^{'}, E) = \int Q(E^{''}, E^{'})G(E^{''}, E)dE^{''} \tag{2}$$

depends on the continuous detector counting $Q(E^{''}, E^{'})$ produced by an incident photon of energy $E^{'}$, and on the broadening due to the detector resolution $G(E^{''}, E)$ centered at the energy E.

Eqn. (2) can be replaced in Eqn. (1) to obtain:

$$I_{measured}(E) = \int \left(\int Q(E^{''}, E^{'})G(E^{''}, E)dE^{''} \right) \varphi(E^{'})I(E^{'})dE^{'}. \tag{3}$$

By exchanging the integration order in both integrals, it is possible to get two integrals that represent the core of this simplified model (Fernandez and Scot, 2009a):

$$I_{measured}(E) = \int U(E^{''})G(E^{''}, E)dE^{''}, \tag{4a}$$

$$U(E^{''}) = \int Q(E^{''}, E^{'})\varphi(E^{'})I(E^{'})dE^{'}. \tag{4b}$$

The integrals can be discretized and solved separately as follows:

$$U(E_s) = \sum_k Q(E_s, E_k^{'})I(E_k^{'})\varphi(E_k^{'}), \tag{5a}$$

$$I_{measured}(E_t) = \sum_s U(E_s)G(E_s, E_t)\ . \tag{5b}$$

* Corresponding author. .
E-mail address: jorge.fernandez@unibo.it (J.E. Fernández).

https://doi.org/10.1016/j.radphyschem.2024.111648
Received 22 December 2023; Received in revised form 21 February 2024; Accepted 26 February 2024
Available online 2 March 2024

$Q(E_s, E_k^{'})$ and $I(E_k^{'})$ in Eqn. (5a) can be computed with a Monte Carlo code while the efficiency $\varphi(E_k^{'})$ needs to be determined independently. The computation of Eqn. (5b) requires the knowledge of the detector resolution $G(E_s, E_t)$.

The model was first tested by using the Monte Carlo code MCSHAPE (Fernandez and Scot, 2009b) with the basic efficiency model in section 2.2 to compute $U(E_s)$, and a symmetric Gaussian distribution for the peak broadening $G(E_s, E_t)$. The $I_{measured}(E_t)$ computed with these approximations shown that the approach is robust but needs improvements to match better the experimental spectrum.

In this paper we analyze and discuss the following improvements to the solution not considered during the first stage.

(a) A better description of the photon transport by including, into the Monte Carlo code, the photons contributed by secondary electrons through the processes of bremsstrahlung and inner shell impact ionization.
(b) A better description of the detector response by including the escape due to Rayleigh scattering into the Monte Carlo code.
(c) A better description of the peak broadening to improve the insufficient description of the symmetric Gaussian distribution.
(d) A better description of efficiency comprising the scattering on the different devices inside the detector walls.
(e) The need to correct the pile-up distortion effects even in case of acquisition with hardware correction.

It will be shown that the model in Eqn. (5) with these improvements is sufficient to give a full description of a complex X-ray spectrum. All the tests will be performed on a synchrotron measurement (Namito et al., 2000) which requires a Monte Carlo code suitable for linearly polarized X-ray photons. It will be shown that an almost perfect description of the measurement is possible even when not all the characteristics of the detector are fully known as in this case.

2. Modeling radiation transport and detector influence

A preliminary description of photon diffusion is obtained as solution of the scalar Boltzmann equation for photons by considering the prevailing interactions in the X-ray regime (characteristic lines produced by atom relaxation after photoelectric effect, Compton scattering and Rayleigh scattering). A more refined description adds the influence of the electron photon coupling to include the contribution of bremsstrahlung, inner shell impact ionization and Compton ionization. The level of detail of such descriptions represents an acceptable approximation for most of the applications involving unpolarized sources but it is not adequate for polarized sources. In such a case, it is necessary to consider the influence of the source polarization state and its modification due to the collisions by introducing the Boltzmann-Chandrasekhar equation, a vector equation able to describe the evolution of the polarization state through the multiple collisions (Fernandez, 1999).

Polarized photon transport (neglecting secondary electrons), studied with deterministic methods (Fernandez et al., 1993), is very useful for analyzing the influence of polarization on the photon field, but is limited by the number of calculable collisions and by the geometry required by the analytical solution. A Monte Carlo simulation is a good alternative because it can be used to solve more complicated geometries with a higher number of collisions and can also be used to describe the detector response.

2.1. Monte Carlo code MCSHAPE

MCSHAPE, a Monte Carlo code developed at the University of Bologna, stands out for its ability to simulate the diffusion of photons with arbitrary polarization states, uniquely capturing the evolution of polarization throughout interactions with atoms. Utilizing the Boltzmann-Chandrasekhar 'vector' transport equation, the code represents the photon polarization state through Stokes parameters I, Q, U, and V quantities with intensity dimensions providing physical insights into polarization (Fernandez, 2007). The simulation focuses on the propagation of photons in heterogeneous media, originating from both, polarized (e.g., synchrotron) or unpolarized (e.g., X-ray tubes) sources.

MCSHAPE's modeling assumes that photons exclusively interact within the target, with those escaping into empty space or air subject to absorption but not returning to the target. This model effectively depicts radiation behavior in two media of differing density, where the sample's density vastly exceeds that of the surrounding half-space.

In determining the scattering angle, the code employs a randomized approach based on the phase function of the collision in the center of mass reference system. Subsequently, the outgoing direction undergoes conversion to the laboratory reference system.

Crucially, the polarization model in MCSHAPE involves a matrix kernel to describe the collision term in the vector transport equation. The code adopts a hybrid method for scattering angle selection, wherein the final polar angle is randomly sampled for each collision event from the scalar differential cross-section (isotropic for photoelectric effect, anisotropic for Compton and Rayleigh scattering). The cosine of the scattering angle is derived from a cumulative function built upon the same distributive function used in the scalar representation of the scattering kernel. Consequently, optimization pertains to the intensity component I of the Stokes vector, while components Q, U, and V are computed using weights. The azimuthal angle in the local center of mass reference system is sampled uniformly.

Secondary electrons may also produce photons through two interaction mechanisms: the bremsstrahlung (which produces a continuous photon energy spectrum) and the inner shell impact ionization (ISII) (an inelastic collision which ionizes the interacting atom causing a vacancy in an atomic shell that is filled through a relaxation process). These two electrons' radiative contributions can be introduced as additional contribution terms to the photon field if they are computed externally. In particular, the Bremsstrahlung contributions is relevant to reproduce the background of the X-ray spectrum (Fernandez et al., 2015a).

The simulation model implemented in MCSHAPE has an option to compute the inherent alterations introduced by the detection system in the measured radiation spectrum. To comprehensively address this aspect, the influence of the detector is evaluated in two distinct stages. Initially, the diffusion of incoming photons into the detector is characterized by a transport model dependent on the physical properties of the detector material, including composition, density, and thickness. The present transport model comprises the escape due to Rayleigh scattering not included in previous versions of the MCSHAPE code. This contribution is not detected as scape but produces a small reduction of the detected signal.

As said before, the broadening and energy resolution, intricately linked to the detection mechanism, are delineated using the independent code RESOLUTION (Fernandez et al., 2015b).

2.2. Simple model of efficiency

Detector efficiency stands as a critical parameter in X-ray and gamma-ray spectroscopy, holding paramount importance in various applications. However, the comprehensive understanding of this property is often accompanied by uncertainty, stemming from diverse definitions in literature (Knoll, 2000). These definitions not only hinge on detection instrumentation but also intertwine with measurement techniques, analysis software, and background radiation levels.

Efficiency, encompassing intrinsic, absolute, total, and peak efficiency, delineates the fraction of detected pulses concerning emitted or incident radiation. These metrics play a pivotal role in estimating a detector's count rate under specific measurement conditions. The efficacy of a detector is contingent upon factors such as material

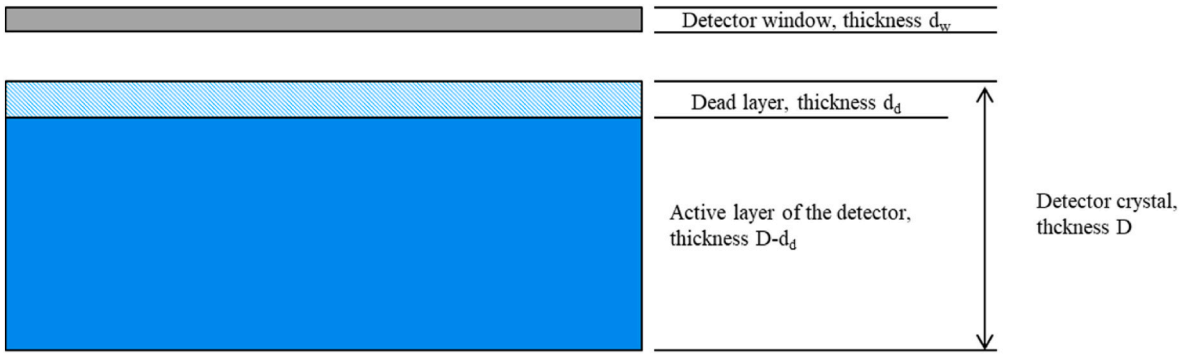

Fig. 1. Simplified representation of a solid-state detector.

composition, geometry, source-detector distance, and the energy of the radiation. In a general sense, all detectors yield an output pulse for each quantum of radiation interacting within their active volume. The process involves primary charged radiation giving rise to interactions, typically ionization or excitation as soon as the particles reach the active volume. After traversing a small fraction of their path, particles lead to sufficient ion-vacancy pairs, ensuring that the resultant pulse is substantial enough to be detected. The efficiency of a detector achieving 100% counting efficiency implies that it can detect all particles entering its active volume. Conversely, when radiation must cover an extensive path between interactions, such as with gamma rays or neutrons, the detector's efficiency is inevitably less than 100%. Therefore, a clear and precise understanding of detector efficiency becomes imperative to establish a link between the number of detected pulses and the incident photons or neutrons.

Absolute efficiency (ε_{abs}) is defined as the ratio of the number of recorded pulses to the number of incident radiation quanta. This ratio is contingent not only on detector properties but also on the characteristics of the geometry used during measurement, primarily the source-detector distance.

$$\varepsilon_{abs} = \frac{n_{number\ of\ pulses\ recorded}}{n_{number\ of\ incident\ radiation\ quanta\ emitted}}$$

This magnitude is reliant not only on the detector's intrinsic properties but also on the specifics of the geometry employed during the measurement, with a particular emphasis on the source-detector distance.

Conversely, intrinsic efficiency (ε_{int}) is defined as the ratio of the number of recorded pulses to the number of incident radiation quanta emitted, incorporating intrinsic detector properties while eliminating the influence of the solid angle subtended by the detector.

$$\varepsilon_{int} = \frac{n_{number\ of\ pulses\ recorded}}{n_{number\ of\ incident\ radiation\ quanta\ emitted\ in\ solid\ angle\ of\ the\ detector}}$$

This metric, in contrast to absolute efficiency, no longer considers the solid angle subtended by the detector as an implicit factor. The intrinsic efficiency of a detector depends on its material composition, the energy of the radiation, and the physical thickness of the detector in the direction of incident radiation. Importantly, it significantly reduces dependence on the source-detector distance.

MCSHAPE incorporates intrinsic efficiency in the computation of the detector response; Focusing on a perpendicularly incident beam, the efficiency $\varphi(E)$ is expressed as:

$$= 1 - e^{\left[-\sum_{i=1}^{N}\frac{\mu_i}{\rho_i}\rho_i s_i\right]}, \tag{6}$$

where N is the number of layers constituting the active detector; and for the i-th layer, μ_i represents the total mass attenuation; ρ_i the density; and s_i the thickness. The quantitative representation of intrinsic efficiency within the MCSHAPE framework is obtained by comprising the attenuation of the beam in the detector window and in the dead layer for the simplified 1D detector shown in Fig. 1:

$$\varphi(E) = \underbrace{exp\ (-\mu_w d_w)}_{attenuation\ in\ the\ the\ window}\ \underbrace{exp\ (-\mu_d d_d)}_{Attenuation\ in\ the\ dead\ layer}\ \underbrace{(1 - exp\ (-\mu_d(D - d_D)))}_{probability\ of\ attenuation\ in\ the\ active\ layer} \tag{7}$$

The dead layer thickness can be estimated experimentally (Maor and Rosner, 1978) and is assumed to be known.

Additionally, it was accomplished an estimation of the potential contribution of scattered radiation in the walls of an 3D detector to the efficiency curve. It was determined that the contribution of reflected radiation is negligible compared to the incident radiation, with a calculated influence of 1.56% for a detector of CdTe of known internal geometry. This finding leads to conclude that reflected radiation can be assumed irrelevant also for a Ge detector. Even when considering the considerable complexity involved in efficiency calculations of real 3D geometries, reflected radiation would yield only a marginal impact on the overall efficiency determination (Giampieri, 2015).

2.3. Energy resolution

The function $S(E^{''})$ relies on the physical properties of the detector, including geometry, composition, density, and thickness, and can be determined using deterministic or Monte Carlo codes.

Energy resolution, intrinsic to the detector type, deviates from ideal behavior. The Full Width at Half Maximum (FWHM) stands as a commonly used parameter for characterizing energy resolution. It is defined as the FWHM of a single energy peak divided by the peak centroid and is expressed as a percentage.

2.3.1. Gaussian resolution

Imperfect energy resolution stems from various sources of fluctuation, including operational drift, random noise, and statistical noise. The discrete nature of measurements introduces statistical noise, depicted as a Gaussian distribution:

$$G(E^{''}, E) = \frac{A}{\sigma\sqrt{2\pi}} e^{-\frac{(E^{''}-E)^2}{2\sigma^2}} = 0.939\frac{A}{FWHM} e^{-2.773\frac{(E^{''}-E)^2}{FWHM^2}}, \tag{8}$$

where $\sigma \approx \frac{FWHM}{2.355}$; E represents the centroid; and A represents the peak area.

However, due to the non-independence of processes within the detector, the resolution computed through purely statistical methods is notably lower than the observed. The combination of statistical noise, electronic noise, and operational drift contributes to the overall energy resolution, appropriately represented by a Gaussian function with FWHM given by:

$$FWMH_{overall} = \sqrt{(FWHM)^2_{statistical} + (FWHM)^2_{noise} + (FWHM)^2_{drift}}\,. \quad (9)$$

2.3.2. HYPERMET resolution

In specific instances, particularly with Solid-State Detectors (SSD), deviations from the ideal Gaussian line shape may occur, manifesting as skewed profiles with elongated tails from the peak centroid to zero energy. To rectify this, corrective models are essential. Charge carrier trapping and incomplete collection (Phillips and Marlow, 1976; Campbell and Maxwell, 1997; Campbell et al., 1985), can lead to count deductions from the full energy peak, resulting in an exponential distribution denoted as:

$$T(i_0, i) = \begin{cases} H_D e^{\left(\frac{i_0 - i}{\alpha}\right)}, i \le i_0 \\ 0, i > i_0 \end{cases} \quad (10)$$

where H_D corresponds to the amplitude of the tail; i corresponds to the channel; and i_0 corresponds to the full energy line channel.

The process of gathering electric charge and the presence of electronic noise can lead to a Plateau, extending from the central point of the peak to zero energy. The plateau is represented with the function $M(i_0, i)$ in which the parameter H_S correspond to the height of the plateau (Fernandez et al., 2015b).

The convolution of $T(i_0, i)$ and $M(i_0, i)$ with the Gaussian distribution produces the shelf and the tail functions:

$$S(i_0, i) = \frac{1}{2} H_S \, erfc\left(\frac{i - i_0}{\sigma\sqrt{2}}\right) \quad (11)$$

$$D(i_0, i) = \frac{1}{2} H_D \, e^{\left(\frac{i - i_0}{\alpha}\right)} \, e^{\left(\frac{\sigma^2}{2\alpha^2}\right)} erfc\left(\frac{i - i_0}{\sigma\sqrt{2}} + \frac{\sigma}{\alpha\sqrt{2}}\right) \quad (12)$$

The parameters H_D, H_S, and α, referred to as HYPERMET parameters, are energy dependent. There exist different computer codes which compute the HYPERMET correction (Fazekas et al., 1997; Fernandez et al., 2015b; Ménesguen and Lépy, 2021).

2.3.3. RESOLUTION code

RESOLUTION is a software tool designed to incorporate the impact of energy resolution smearing and incomplete charge collection into simulated X-ray and gamma-ray spectra, reflecting the energy deposition spectrum within the detector. The using algorithm utilizes a modified model of Campbell (Campbell et al., 1985) to express SF(E), representing the shelf fraction, TF(E), representing the tail fraction and β proper of the model. The fitting parameters used to define the three coefficients of the model depend on the specific detector and are empirically determined (Campbell and Maxwell, 1997). In the RESOLUTION algorithm (Fernandez et al., 2015b), the parameters HS and HD in the HYPERMET function are derived from SF and TF through the incorporation of appropriate normalization factors.

2.4. Pile-up correction of the measurement

Radiation emission is a process randomly spaced in time. At high counting rates pulses may have time gap smaller than their width, giving place to the pulse pile-up. It has three consequences: loss of counts (since the sum of the pulses is detected instead of the separate pulses) and wrong energies of the piled-up pulses. Therefore, the whole spectrum results distorted since the lost pulses are not collected at the proper energies. Modern detectors usually comprise built-in electronics which partially reduce pile-up effects either by limiting the pulse tail (i.e. Rise Time Discrimination, RTD) and/or by using additional rejection circuits. It is worth mentioning that PPU is exclusively attributed to the detector's pulse handling circuitry and is not related to the detector response function.

The Deterministic Rectangular Pulse Pile-Up (DRPPU) method addresses the correction of residual pulse pile-up (PPU) in radiation detectors even after PPU reduction circuitry. DRPPU introduces a first-principles balance equation for second order PPU, offering a post-processing correction for X-ray measurements. Specifically applied to rectangular pulse shapes, the method employs a deterministic iterative procedure with demonstrated convergence. In essence, DRPPU serves as an efficient corrective measure for mitigating the impact of pulse pile-up distortions in radiation detector measurements (Sabbatucci and Fernandez, 2017).

Table 1
Ge detector and FWHM parameters.

Thickness (cm)	0.1
Density (g/cm3)	8.92
W (keV)	2.9600000E-03
F	5.9999999E-02
a (keV)	1.0000000E-06
b	2.000000
ΔE_{elec} (keV)	0.2500000

3. Results and discussion

3.1. Description of the measure

In the reference measure, a mono-energy photon-scattering experiment was conducted at the BL-14C beamline of a 2.5 GeV synchrotron light facility. Utilizing photons from a vertical wiggler and a Si (1,1,1) double crystal monochromator, a linearly polarized mono-energy photon beam was generated. The experimental set-up is described in (Namito et al., 2000). The data that we have are relative to carbon and copper (Y. Namito and H. Hirayama, Private communication with raw experimental data from KEK synchrotron). In this work only the copper spectrum will be considered. The source is linearly polarized with linear polarization degree P = 0.885. The source energy is 40 keV. To see the effect of the polarization, the scattered spectrum is collected by two Ge detectors. One Ge detector (Ge2) was in the plane of the incident polarization vector ($\varphi = 0°$), and the other (Ge1) in the plane perpendicular to it ($\varphi = 90°$). The scattering angle is $\theta = 90°$. This set-up was simulated by MCSHAPE v. 271. Since the code can represent only 1D geometries, for each target two runs of the code were performed to repeat the experimental conditions. For each run, the incoming and the take-off angles are both 45°. The azimuthal angle is 0°. The detector is assumed to be a Ge layer of 1 mm thickness. For the Ge1 situation, the source considered is linearly polarized in the plane perpendicular to the scattering one, while for the Ge2 situation we use a source with linear and parallel polarization respect to the scattering plane.

3.2. Steps to describe the experimental X-Ray spectrum

A two stage MCSHAPE calculation is performed. In the first stage (transport), the code simulates the transport of the photons in the target; the resulting emerging spectrum is scored. Please note the improvement in the background description of MCSHAPE when the photon transport

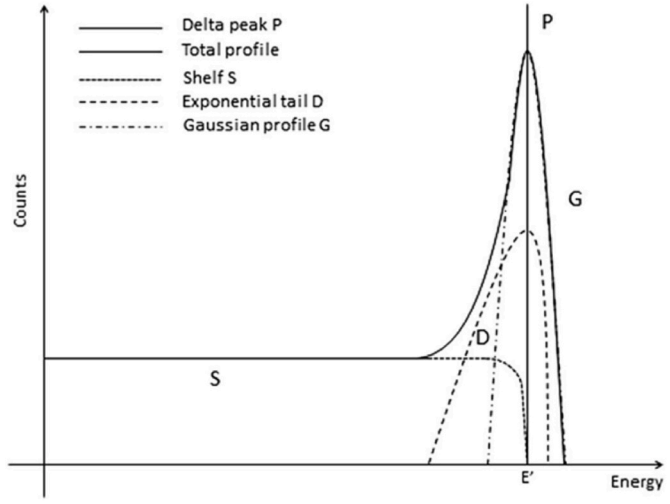

Fig. 2. Different functions which contribute to the description of a single peak under the HYPERMET model.

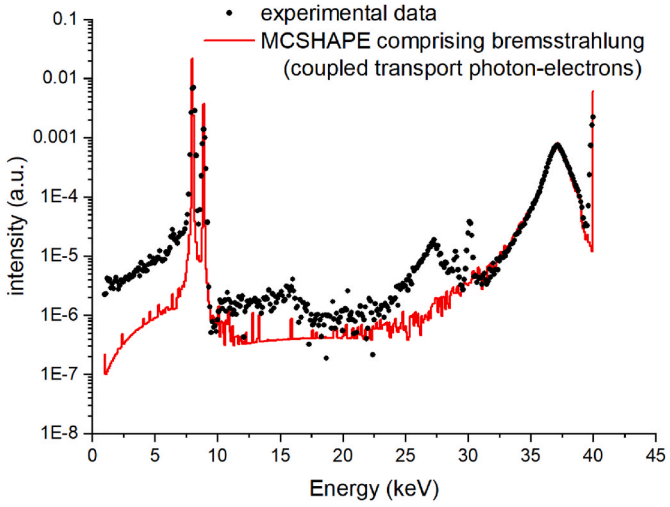

Fig. 3. MCSHAPE spectrum simulation comprising contributions from photon-electron coupling.

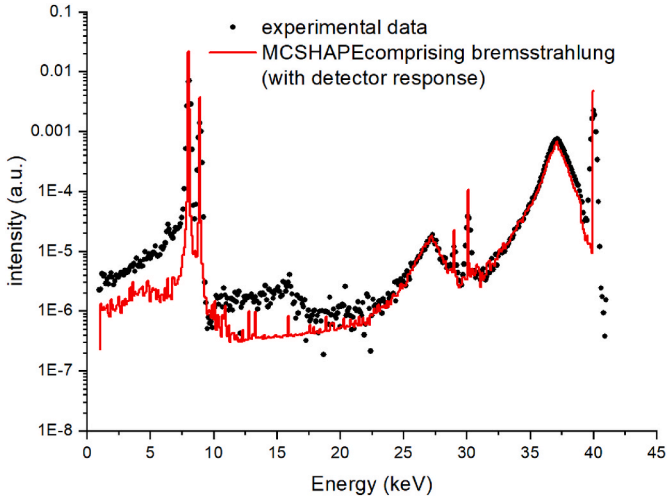

Fig. 4. MCSHAPE spectrum simulation comprising detector response without the peak broadening due to detector resolution.

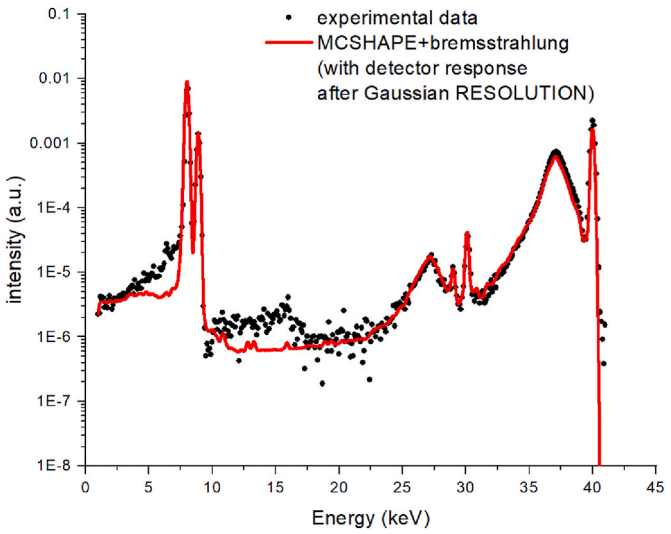

Fig. 5. MCSHAPE spectrum simulation comprising detector response with Gaussian broadening computed with the code RESOLUTION.

Table 2
HYPERMET parameters used in the RESOLUTION code.

c_0	7.000000	α parameter
c_1	0.0000000 E+00	
c_2	0.0000000 E+00	$\alpha = c_0 + c_1 E + c_2 E^2 + c_3 E^3$
c_3	0.0000000 E+00	
b_0	1.5000000E-02	Tail fraction
b_1	9.9999997E-06	
b_2	0.0000000 E+00	$TF = b_0 \exp(b_1 E) + b_2 \exp(b_3 E)$
b_3	3.0000001E-06	
a_0	4.9999999E-03	Shelf fraction
a_1	0.0000000 E+00	
a_2	0.0000000 E+00	$SF = a_0 + a_1 \exp(a_2 E)$

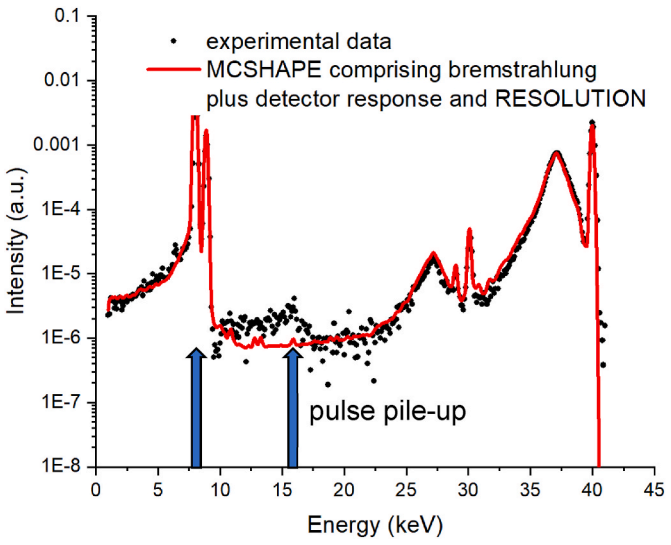

Fig. 6. MCSHAPE spectrum simulation comprising the detector response and the HYPERMET broadening computed with the code RESOLUTION. The unexplained part of the spectrum located at 16 keV can be ascribed to pile up (right arrow) of the Cu K-lines (left arrow) having half of the energy.

includes the photons contributed by secondary electrons through the processes of bremsstrahlung and inner shell impact ionization. Bremsstrahlung is responsible for the continuous background. Even if the extent is not high, it has a big visual impact on the spectrum description

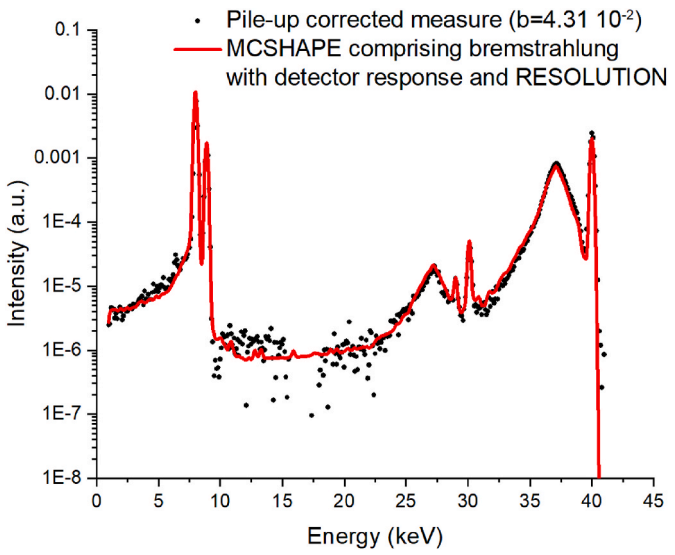

Fig. 7. Simulation matches the experimental spectrum after the pile-up correction.

(Fernandez et al., 2015a).

In the second stage MCSHAPE computation (detector response function), the output of the transport run is used as source and the detector as target. In this case a better description of the detector response is obtained by including into the Monte Carlo the escape due to Rayleigh scattering. The simplified model described by Eqn. (7) in section 2.2 is sufficient to characterize the efficiency since the influence of multiple scattering inside the walls of the detector is negligible. The beam is supposed to hit perpendicularly in the middle of the detector. The output of this second stage is the spectrum including the detector response function (see Fig. 4).

The postprocessing code RESOLUTION is then used to add the energy resolution of the detector. Table I shows the parameters used to calculate the FWHM for the Ge detector.

Firstly, it is assumed a Gaussian distribution (see Fig. 5). The spectrum description is insufficient, especially in relation to the Cu lines under 10 keV. It is apparent the bad description of the low energy tail of the peaks.

The next step consists in determining experimentally the HYPERMET parameters for the code RESOLUTION. This operation usually requires the measure of single isolated peaks at different energies to reach a definitive detector characterization. In absence of such a set of measurements, the HYPERMET parameters in RESOLUTION are obtained by using the measurement itself. The two low energy Cu K peaks and the Rayleigh peak at 40 keV allow to determine the set of RESOLUTION parameters (see Table 2).

With these parameters it is possible to obtain the spectrum in Fig. 6. It is apparent the good description in the whole energy range except for the peak near 15 keV which can be considered the pile-up of the two characteristic peaks of Cu lying at half of the energy.

Pile-up distortion is frequently present in radiation measures even in the case of acquisition with hardware correction and need to be corrected with adequate software. Fig. 7 shows the previous experimental measurement post-corrected with the code DRPPU (Sabbatucci and Fernandez, 2017) to reduce the pile-up effects. After the PPU correction, the simulation matches almost perfectly the resulting experimental data.

4. Conclusions

The representation of an X-ray fluorescence spectrum requires an adequate model to describe the modifications of the detection system on the measurement. The mathematical model described by Eqn. (4) represents a simple and robust answer. The practical application to a measurement requires the use of the discretized set of Eqn. (5). The complexity of the problem requires that the pieces involved must fulfill the following stringent conditions: to use an adequate transport simulation tool capable of describing the physics to a higher extent; to perform an adequate simulation of the detector response; to describe well the detector efficiency; to describe well the resolution of the detector; and sometimes you discover that pulse pile-up is still present and

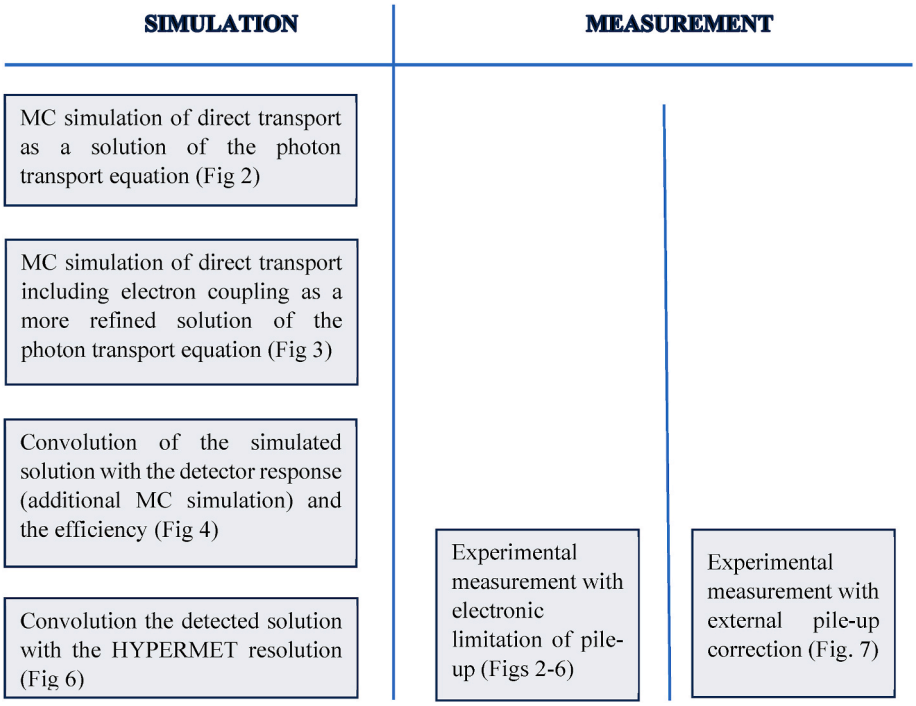

Fig. 8. Steps illustrated in Section 3 to obtain the final guess in Fig. 6. Figs. 2–6 show comparisons with raw experimental data. Fig. 7 shows the comparison of the final simulation stage with experimental data after recovering from pile-up.

needs to be corrected a posteriori.

For both, the simulation of the direct photon transport and for the detector response, it was used the Monte Carlo 1-D code MCSHAPE v271 which is suitable to describe the photon transport of sources with arbitrary states of polarization. The transport simulation has been corrected to include coupled electron-photon contributions like bremsstrahlung and inner shell impact ionization. A second step of the same MC code is used to simulate the detector response. The simple model given by Eqn (7) is sufficient to describe the detector efficiency since multiple scattering inside the detector walls computed with a 3-D MC code is negligible. The most important correcting piece is the peak anisotropy in the RESOLUTION postprocessing. The inclusion of the HYPERMET parameters has demonstrated to be fundamental for obtaining a better result. The spectrum obtained after these corrections clearly shown the presence of pile up peak; therefore, it was necessary to apply a post-processing pile-up reduction. The simulation steps are summarized in Fig. 8.

It has been shown that the general model represented by Eqn. (4) is adequate; the addition of the described set of corrective steps helps to reach excellent results; and the corrections can be performed even with incomplete knowledge of the detector.

The practical application of the corrections requires the use of different simulation codes like MCSHAPE, RESOLUTION and DRPPU. In the future it is expected to complete the integration of all the corrective steps in a unique piece of software.

CRediT authorship contribution statement

Jorge E. Fernández: Writing – review & editing, Writing – original draft, Supervision, Software, Investigation, Conceptualization. **Gianmarco Grippo:** Writing – review & editing, Writing – original draft, Investigation, Data curation. **Francesco Teodori:** Investigation. **Viviana Scot:** Validation, Software, Investigation, Data curation.

Declaration of competing interest

The authors declare that they have no known competing financial interests or personal relationships that could have appeared to influence the work reported in this paper.

Data availability

Data will be made available on request.

References

Campbell, J.L., Maxwell, J.A., 1997. A cautionary note on the use of the Hypermet tailing function in X-ray spectrometry con Si(Li) detectors. Nucl. Instrum. Methods Phys. Res. Sect. B Beam Interact. Mater. Atoms 129, 297–299. https://doi.org/10.1016/S0168-583X(97)00229-2, 1997.

Campbell, J.L., Millman, B.M., Maxwell, J.A., Perujo, A., Teesdale, W.J., 1985. Analytic fitting of monoenergetic peaks from Si(Li) X-ray spectrometers. Nucl. Instrum. Methods Phys. Res. Sect. B Beam Interact. Mater. Atoms 9 (1), 71–79. https://doi.org/10.1016/0168-583X(85)90780-3. Apr. 1985.

Fazekas, B., Molmir, G., Beigya, T., Dabolczi, L., Simonits, A., 1997. Introducing HYPERMET-PC for automatic analysis of complex gamma-ray spectra. J. Radioanal. Nucl. Chem. 215 (No. 2), 271–277. https://doi.org/10.1007/bf02034477, 1997.

Fernandez, J.E., 1999. Polarisation effects in multiple scattering photon calculations using the Boltzmann vector equation. Radiat. Phys. Chem. 56 (1), 27–59. https://doi.org/10.1016/S0969-806X(99)00287-X. Aug. 1999.

Fernandez, J.E., 2007. Multiple scattering of photons using the Boltzmann transport equation. Nucl. Instrum. Methods Phys. Res. Sect. B Beam Interact. Mater. Atoms 263 (1), 7–21. https://doi.org/10.1016/j.nimb.2007.04.171. Oct. 2007.

Fernandez, J.E., Scot, V., 2009a. Simulation of the detector response function with the code MCSHAPE. Radiat. Phys. Chem. 78 (10), 882–887. https://doi.org/10.1016/j.radphyschem.2009.04.018. Oct. 2009.

Fernandez, J.E., Scot, V., 2009b. Simulation of the detector response function with the code MCSHAPE. Radiat. Phys. Chem. 78 (10), 882–887. https://doi.org/10.1016/j.radphyschem.2009.04.018. Oct. 2009.

Fernandez, J.E., Hubbell, J.H., Hanson, A.L., Spencer, L.V., 1993. Polarization effects on multiple scattering gamma transport. Radiat. Phys. Chem. 41 (4), 579–630. https://doi.org/10.1016/0969-806X(93)90316-M. Apr. 1993.

Fernandez, J.E., Scot, V., Di Giulio, E., Salvat, F., 2015a. Bremsstrahlung contribution to the X-ray spectrum in coupled photon–electron transport. X Ray Spectrom. 44 (4), 248–254. https://doi.org/10.1002/xrs.2615, 2015.

Fernandez, J.E., Scot, V., Sabbatucci, L., 2015b. A modeling tool for detector resolution and incomplete charge collection. X Ray Spectrom. 44 (3), 177–182. https://doi.org/10.1002/xrs.2597. May 2015.

Giampieri, A., 2015. Caratterizzazione della funzione risposta di un detector CdTe mediante simulazione Monte Carlo, Nov. 2015. In: Italian (Ed.), Nuclear Engineering Master Thesis. University of Bologna. https://doi.org/10.13140/RG.2.1.3221.1288, 2015.

Knoll, G.F., 2000. Radiat. Detect. Measure, third ed. John Wiley & Sons, New York. 2000. ISBN: 0-471-07338-5.

Maor, D., Rosner, B., 1978. Efficiency of Ge and Si(Li) detectors at very low energies by an X-ray doublet method. J. Phys. E: Sci. Instrum 11 (11), 1141. https://doi.org/10.1088/0022-3735/11/11/016. Nov. 1978.

Ménesguen, Y., Lépy, M.-C., 2021. COLEGRAM, a flexible user-friendly software for processing of ionizing radiation spectra. Nucl. Instrum. Methods Phys. Res. Sect. A Accel. Spectrom. Detect. Assoc. Equip. 1003 (2021), 165341 https://doi.org/10.1016/j.nima.2021.165341.

Namito, Y., Hirayama, H., Ban, S., 2000. Improvements of low energy photon transport for EGS5. (KEK-PROC-2000-20). In: Ban, S. (Ed.), Proceedings of the Second International Workshop on EGS. Japan.

Phillips, G.W., Marlow, K.W., 1976. Automatic analysis of gamma-ray spectra from germanium detectors. Nucl. Instrum. Methods 137 (3), 525–536. https://doi.org/10.1016/0029-554X(76)90472-9. Sep. 1976.

Sabbatucci, L., Fernandez, J.E., 2017. First principles pulse pile-up balance equation and fast deterministic solution. Radiat. Phys. Chem. 137, 12–17. https://doi.org/10.1016/j.radphyschem.2016.09.014. Aug. 2017.

Seltzer, S.M., 1981. Calculated response of intrinsic germanium detectors to narrow beams of photons with energies up to ~300 keV. Nucl. Instrum. Methods Phys. Res. 188 (1), 133–151. https://doi.org/10.1016/0029-554X(81)90332-3. Sep. 1981.